AIAA JOURNAL
Vol. 36, No. 7, July 1998

Static and Dynamic Aeroelasticity of Advanced Aircraft Wings Carrying External Stores

Frank H. Gern* and Liviu Librescu†
Virginia Polytechnic Institute and State University, Blacksburg, Virginia 24061-0219

A study of the static and dynamic aeroelasticity of aircraft wings carrying external stores is presented. The wing structure is modeled as a laminated composite plate exhibiting flexibility in transverse shear and including warping restraint effects. The relevant equations of motion and boundary conditions are obtained via Hamilton's variational principle and application of generalized function theory. To achieve a realistic representation of the store influence on static and dynamic behavior of the system, static weights, as well as dynamic inertias of the stores, are considered. For the problem at hand, three-dimensional strip theory aerodynamics is employed. The obtained eigenvalue/boundary value problems are being solved by application of the extended Galerkin method. The solution procedure is used to investigate the implications of external stores on static aeroelastic response, divergence, free vibration, and flutter. Comparisons with the very few results highlighting the effects of underwing and tip stores on flutter instability are carried out, and excellent agreements with the present predictions are reported.

Nomenclature

a_0 = sectional lift-curve slope
b = wing semichord length, $c/2$
$C(k)$ = Theodorsen function, $F(k) + iG(k)$
c = wing chord length measured perpendicular to the reference axis
E = in-plane Young's modulus
E_p = distance between center of gravity of store and wing elastic axis, positive aft
$F_i^{(m,n)}$ = generalized body forces of order (m, n); Eq. (11)
f = frequency of oscillation
f_2, g_2 = displacement measures; Eq. (2a)
G', G_{12} = transverse shear modulus, in-plane shear modulus
g = gravity acceleration
h = plunging displacement, positive upward
$I^{(m,n)}$ = generalized mass terms of order (m, n); Eq. (11)
K_p = pitching radius of gyration of the store about its center of gravity
k = reduced frequency, $\omega b/V_n = \omega b/(V\cos\Lambda)$
$\mathcal{L}$ = sectional lift, positive upward
l = wing semispan measured along the reference axis
$\mathcal{M}$ = sectional aerodynamic torque about wing elastic axis, positive nose up
$\bar{Q}_{ij}$ = modified components of the elasticity tensor
q_n = component of the dynamic pressure normal to the reference axis, $\rho V_n^2/2$
R = transverse shear flexibility parameter, E/G'
$T_{ij}^{(m,n)}$ = generalized stress couples of order (m, n); Eq. (10)
U_i = components of the three-dimensional displacement vector; Eq. (1)
V, V_n = airstream velocity and its component normal to the reference axis
x_0 = elastic axis position measured from the reference axis, positive aft
x_1, x_2, x_3 = chordwise, spanwise, and transverse coordinate normal to the midplane of the wing, respectively
δ, δ_D = variation operator, Dirac operator
ε = E_p/c
η, η_w = x_2/l, nondimensional spanwise location of wing store
θ, θ_0 = elastic twist angle, prescribed rigid-wing angle of attack
Λ = sweep angle of the reference axis, positive for sweptback
λ, λ_F = speed parameter $(V/b\omega_h)$, flutter speed parameter $(V_F/b\omega_h)$
μ_T, μ_w = $m_{\text{tipstore}}/m_{\text{wing}}, m_{\text{wingstore}}/m_{\text{wing}}$
ν = Poisson's ratio
Ω, Ω_F = frequency parameter, ω/ω_h; flutter frequency parameter, ω_F/ω_h
ω = circular frequency of oscillation
$(\,)_{,2}, (\,)'$ = $\mathrm{d}(\,)/\mathrm{d}x_2, \mathrm{d}(\,)/\mathrm{d}\eta$

Subscripts

S, W, T = stores, wing, tip store

Introduction

FUTURE design concepts of civil and military aircraft are likely to imply the achievement of extremely lightweight structural configurations. With weight savings and performance gaining ever increasing importance, the next generation of flight vehicles will exhibit increased structural flexibility. One outstanding example for the realization of huge airframes exhibiting high flexibility of wings and fuselage is the new ultra high capacity aircraft (UHCA) envisaged to be realized by American and European commercial aircraft manufacturers. With expected wing tip bending deflections of up to 3 m, the structural and aeroelastic design of UHCA becomes a major and challenging problem.[1]

In addition, future advanced flight vehicle structures are likely to be fabricated of advanced composite materials. In contrast to metallic structures, their composite counterparts exhibit exotic features whose effects on the aeroelastic behavior have to be carefully investigated and perfectly understood. The possibilities of beneficially tailoring the aeroelastic properties of advanced wing structures by the employment of composite materials have recently been pointed out by some recognized aeroelasticians, e.g., Ref. 2, and were successfully demonstrated by the development of the Grumman X-29 forward swept wing aircraft. Nevertheless, nonclassical and very often detrimental effects such as warping inhibition and transverse shear flexibility of constituent materials are important effects that have to be included in the structural model.[3]

Inasmuch as modern aircraft wings are very often designed to carry external stores, this item has gained special importance in the

Received Nov. 13, 1997; revision received March 27, 1998; accepted for publication March 28, 1998.

*DFG Research Fellow, Department of Engineering Science and Mechanics. Member AIAA.
†Professor, Department of Engineering Science and Mechanics.

consideration of wing aeroelasticity. In the case of transport aircraft, these are mostly underwing carried stores such as large and heavy engines, fuel tanks, or tip stores such as winglets.[4] Store attachments to fighter aircraft wings range within a wide variety of tank and missile configurations.[5] Keeping in mind that the tremendous variety of store configurations and spanwise arrangements may dramatically influence static and dynamic aeroelasticity of aircraft wings, the study of this problem has received prominence only two decades ago.[6] Because it is known that pylon-mounted stores strongly influence dynamic wing characteristics, the store pitching modes are of special importance from an aeroelastic point of view.[7] With store pitching modes being in the proximity of the wing's fundamental bending frequency, critical aeroelastic coupling of the modes may occur, commonly referred to as wing-with-stores flutter. To the authors' knowledge, the major body of literature in this area is devoted to metallic wings, mainly unswept wing structures,[5–9] with few studies dealing with composite wings.[10,11]

These facts imply that reliable analysis and design of advanced high-performance flight vehicles necessitate the development of a refined simulation model featuring the incorporation of a number of important effects, such as anisotropy and nonhomogeneity of the constituent composite materials, nonclassical effects exhibited by advanced composite structures, and the presence of external stores attached to the wing structure. To get pertinent information of the influence of the mentioned effects and to determine the aeroelastic capabilities of the design, parametric studies, which are essential during the preliminary design phases of the flight vehicle, have to be conducted. The present work provides the basis for the accomplishment of such studies.

Structural Modeling

To investigate the effects of wing-mounted stores on the aeroelasticity of advanced aircraft wings, a comprehensive structural model has been developed. Based on the concept of a shear deformable plate-beam model, the wing structure is idealized as a laminated composite plate, each constituent layer featuring different ply angles, material, and thickness properties. The total number of layers is N. The reference plane of the composite structure is selected to coincide with the plane interface between the two contiguous layers r and $r+1$ ($1 \le r \le N$). Its points are referred to a Cartesian system of in-plane coordinates (x_1, x_2). The coordinate x_3 is normal to the plane (x_1, x_2), its positive direction being upward (Fig. 1). The x_1 and x_2 coordinates are the chordwise and spanwise coordinates, respectively, whereas the reference plane is defined by $x_3 = 0$.

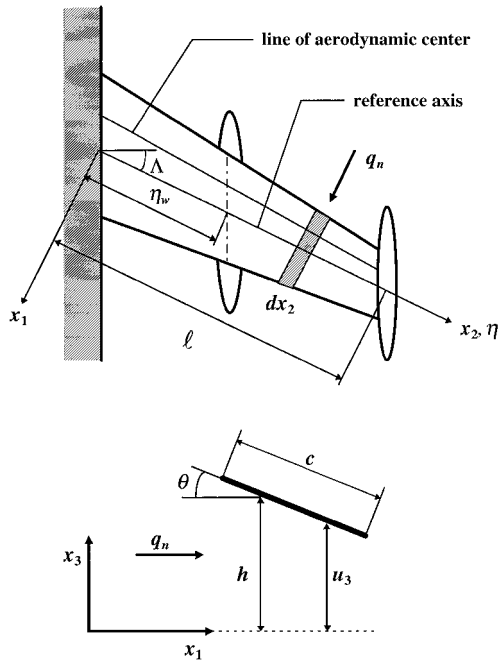

Fig. 1 Geometry of the swept composite wing carrying external stores.

The structural model is developed by postulating the chordwise nondeformability, as well as the following representation of the three-dimensional displacement components:

$$U_1(x_1, x_2, x_3; t) = u_1(x_1, x_2; t) + x_3\psi_1(x_1, x_2; t) \tag{1a}$$

$$U_2(x_1, x_2, x_3; t) = u_2(x_1, x_2; t) + x_3\psi_2(x_1, x_2; t) \tag{1b}$$

$$U_3(x_1, x_2, x_3; t) = u_3(x_1, x_2; t) \tag{1c}$$

Here (u_1, u_2, u_3) are the displacement components along the (x_1, x_2, x_3) coordinates and are associated with the points of the reference plane of the composite panel ($x_3 = 0$); ψ_1 and ψ_2 are the angles of rotation of a line element originally normal to the reference plane about the axes x_2 and x_1, respectively, and t is the time variable. Equations (1), well known in the modeling of shear deformable plate and shell theories, correspond to the first-order transverse shear deformation theory (see, e.g., Ref. 12). To reduce the three-dimensional problem of the wing structure to an equivalent one-dimensional one, it is postulated that

$$\psi_2(x_1, x_2; t) = f_2(x_2; t) + x_1 g_2(x_2; t) \tag{2a}$$

$$u_3(x_1, x_2; t) = h(x_2; t) - (x_1 - x_0)\theta(x_2; t) \tag{2b}$$

Equation (2b) describes the vertical displacement of a wing of rigid cross sections, where $h(x_2; t)$ is the plunging displacement (positive upward) of the wing cross sections measured at the elastic axis, located at $x_1 = x_0$ ($\equiv x_0(x_2)$). As a result, Eqs. (1) become

$$U_1 = x_3\theta(x_2; t) \tag{3a}$$

$$U_2 = u_2(x_2; t) + x_3[f_2(x_2; t) + x_1 g_2(x_2; t)] \tag{3b}$$

$$U_3 = h(x_2; t) - (x_1 - x_0)\theta(x_2; t) \tag{3c}$$

Consistent with Eqs. (3), the strain components e_{ij} are[13]

$$e_{11} = U_{1,1} = 0 \tag{4a}$$

$$e_{22} = U_{2,2} = u_{2,2} + x_3(f_{2,2} + x_1 g_{2,2}) \tag{4b}$$

$$\gamma_{12}\ (\equiv 2e_{12}) = U_{1,2} + U_{2,1} = x_3(\theta_{,2} + g_2) \tag{4c}$$

$$e_{33} = U_{3,3} = 0 \tag{4d}$$

$$\gamma_{13}\ (\equiv 2e_{13}) = U_{1,3} + U_{3,1} = 0 \tag{4e}$$

$$\gamma_{23}\ (\equiv 2e_{23}) = f_2 + x_1 g_2 + h_{,2} - x_1\theta_{,2} + (x_0\theta)_{,2} \tag{4f}$$

In Eqs. (4) and in the forthcoming development, $(\,)_{,i} \equiv \partial(\,)/\partial x_i$. For $f_2 = -h_{,2} - (x_0\theta)_{,2}$ and $g_2 = \theta_{,2}$, it results that $\gamma_{13} = \gamma_{23} = 0$, which is consistent with the traditional assumption of an infinite stiffness of the wing structure in transverse shear (Kirchhoff's theory).

The relevant equations of motion and appropriate boundary conditions are obtained via Hamilton's variational principle and application of generalized function theory to exactly consider the spanwise location and properties of the attached stores. To achieve a realistic representation of the store influence on static and dynamic behavior of the entire system, static weights, as well as dynamic inertias of rigidly attached stores, are considered, yielding the energy functional of a composite wing carrying external stores:

$$J = \int_{t_0}^{t_1} (\mathcal{U}_W - \mathcal{K}_W + \mathcal{A}_W - \mathcal{K}_S + \mathcal{A}_S)\,\mathrm{d}t \tag{5}$$

In Eq. (5) $\mathcal{U}$ is the strain energy, $\mathcal{K}$ the kinetic energy, and $\mathcal{A}$ the potential energy of body and surface forces. The indices W and S identify the affiliation of the various quantities to wing and external stores, respectively. From the stationary condition $\delta J = 0$, consistent with Eq. (5) and adopting the Einstein summation convention, one obtains

$$\delta J = 0 = \int_{t_0}^{t_1} \mathrm{d}t \underbrace{\left\{\left[-\int_\tau \sigma_{ij}\delta U_{i,j}\,\mathrm{d}\tau + \int_\tau \rho(H_i - \ddot{U}_i)\delta U_i\,\mathrm{d}\tau + \int_{\Omega_\sigma} \sigma_i \delta \underset{\sim}{U}_i\,\mathrm{d}\Omega\right]\right.}_{\text{wing}}$$

$$\underbrace{\left. + \sum_s \int_0^l \delta_D\big(x_2 - x_2^{(s)}\big)\left[-\int_{\tau_s} \rho^{(s)}\ddot{U}_i^{(s)}\delta U_i^{(s)}\,\mathrm{d}\tau + \mathcal{L}^{(s)}\delta h^{(s)} - \mathcal{M}^{(s)}\delta\theta^{(s)} + m^{(s)}\delta U_3^{(s)}\right]\mathrm{d}x_2\right\}}_{\text{external stores}} \tag{6}$$

In Eq. (6), the superposed dots denote time derivatives. The terms underscored by a tilde are prescribed quantities. For a straight wing, the pitching angle $\theta^{(s)}$ of the stores coincides with the wing pitching angle θ. To consider swept wings, the three-dimensional displacement quantities of the stores have to be referred to the wing coordinate system to express the stores' main inertia properties that are in chordwise direction. This transformation yields

$$U_1^{(s)} = x_3\theta\cos\Lambda - u_2\sin\Lambda - x_3(f_2 + x_1 g_2)\sin\Lambda \tag{7a}$$

$$U_2^{(s)} = x_3\theta\sin\Lambda + u_2\cos\Lambda + x_3(f_2 + x_1 g_2)\cos\Lambda \tag{7b}$$

$$U_3^{(s)} = h - (x - x_0)[\theta\cos\Lambda - f_2\sin\Lambda - x_1 g_2\sin\Lambda] \tag{7c}$$

Employing the displacement and strain components from Eqs. (3) and (4) and performing the indicated mathematical operations, the explicit form of Eq. (6) for the case of a composite aircraft wing carrying external stores is

$$\delta J = 0 = \int_{t_0}^{t_1} \mathrm{d}t \underbrace{\left\{\int_0^l [A_1\delta u_2 + A_2\delta f_2 + A_3\delta g_2 + (A_4 - \mathcal{M})\delta\theta + (A_5 + \mathcal{L})\delta h]\,\mathrm{d}x_2 + A_6\right.}_{\text{energy functional of the clean composite wing}}$$

$$- \sum_s m^{(s)}\delta_D\big(x_2 - x_2^{(s)}\big)\big\{(\ddot{u}_2 + x_3\ddot{f}_2 + x_1 x_3\ddot{g}_2)\delta u_2 + \big[x_3\ddot{u}_2 + \big(x_3^2 + K_p^{2(s)}\sin^2\Lambda\big)\ddot{f}_2 + \big(x_1 x_3^2 + x_1 K_p^{2(s)}\sin\Lambda\big)\ddot{g}_2$$

$$- K_p^{2(s)}\ddot{\theta}\sin\Lambda\cos\Lambda - E_p^{(s)}\ddot{h}\sin\Lambda\big]\delta f_2 + x_1\big[x_3\ddot{u}_2 + \big(x_3^2 + K_p^{2(s)}\sin^2\Lambda\big)\ddot{f}_2 + \big(x_1 x_3^2 + x_1 K_p^{2(s)}\sin\Lambda\big)\ddot{g}_2$$

$$- K_p^{2(s)}\ddot{\theta}\sin\Lambda\cos\Lambda - E_p^{(s)}\ddot{h}\sin\Lambda\big]\delta g_2 + \big[-K_p^{2(s)}\ddot{f}_2\sin\Lambda\cos\Lambda - x_1 K_p^{2(s)}\ddot{g}_2\sin\Lambda\cos\Lambda + \big(x_3^2 + K_p^{2(s)}\cos^2\Lambda\big)\ddot{\theta}$$

$$\underbrace{+ E_p^{(s)}\ddot{h}\cos^2\Lambda\big]\delta\theta + \big(-E_p^{(s)}\ddot{f}_2\sin\Lambda - x_1 E_p^{(s)}\ddot{g}_2\sin\Lambda + E_p^{(s)}\ddot{\theta}\cos\Lambda + \ddot{h}\big)\delta h\big\}}_{\text{kinetic energy of external stores}}$$

$$\underbrace{+ \sum_s \delta_D\big(x_2 - x_2^{(s)}\big)\big[\mathcal{M}^{(s)}\sin\Lambda\delta f_2 + x_1\mathcal{M}^{(s)}\sin\Lambda\delta g_2 - \mathcal{M}^{(s)}\cos\Lambda\delta\theta + \mathcal{L}^{(s)}\delta h\big]}_{\text{aerodynamic forces acting on external stores}}$$

$$\underbrace{\left. + \sum_s m^{(s)} g\delta_D\big(x_2 - x_2^{(s)}\big)\big[E_p^{(s)}\sin\Lambda\delta f_2 + x_1 E_p^{(s)}\sin\Lambda\delta g_2 - E_p^{(s)}\cos\Lambda\delta\theta + \delta h\big]\right\}}_{\text{potential energy of external stores}} \tag{8}$$

The coefficients A_1–A_6, displayed in Ref. 13, are provided for completeness:

$$A_1 = \big[T_{22,2}^{(0,0)} + F_2^{(0,0)} - I^{(0,0)}\ddot{u}_2 - I^{(0,1)}\ddot{f}_2 - I^{(1,1)}\ddot{g}_2\big] \tag{9a}$$

$$A_2 = \big[T_{22,2}^{(0,1)} - T_{23}^{(0,0)} + F_2^{(0,1)} - I^{(0,1)}\ddot{u}_2 - I^{(0,2)}\ddot{f}_2 - I^{(1,2)}\ddot{g}_2\big] \tag{9b}$$

$$A_3 = \big[T_{22,2}^{(1,1)} - T_{12}^{(0,1)} - T_{23}^{(1,0)} + F_2^{(1,1)} - I^{(1,1)}\ddot{u}_2 - I^{(1,2)}\ddot{f}_2 - I^{(2,2)}\ddot{g}_2\big] \tag{9c}$$

$$A_4 = \big[T_{12,2}^{(0,1)} - T_{23,2}^{(1,0)} + x_0 T_{23,2}^{(0,0)} + F_1^{(0,1)} - F_3^{(1,0)} + x_0 F_3^{(0,0)} - \big(I^{(0,2)} + I^{(2,0)} - 2x_0 I^{(1,0)} + x_0^2 I^{(0,0)}\big)\ddot{\theta} + \big(I^{(1,0)} - x_0 I^{(0,0)}\big)\ddot{h}\big] \tag{9d}$$

$$A_5 = \big[T_{23,2}^{(0,0)} + F_3^{(0,0)} - I^{(0,0)}\ddot{h} + \big(I^{(1,0)} - x_0 I^{(0,0)}\big)\ddot{\theta}\big] \tag{9e}$$

$$A_6 = -\big[T_{22}^{(0,0)}\delta u_2\big]_0^l - \big[T_{22}^{(0,1)}\delta f_2\big]_0^l - \big[T_{22}^{(1,1)}\delta g_2\big]_0^l - \big[T_{23}^{(0,0)}\delta h\big]_0^l - \big[\big(T_{12}^{(0,1)} - T_{23}^{(1,0)} + x_0 T_{23}^{(0,0)}\big)\delta\theta\big]_0^l \tag{9f}$$

In Eqs. (9), the one-dimensional generalized stress couples and the generalized body forces and mass terms of order (m, n), measured per unit span, are defined as

$$T_{ij}^{(m,n)}(x_2) = \int_A \sigma_{ij} x_1^m x_3^n\,\mathrm{d}A \tag{10}$$

$$\begin{Bmatrix} F_i^{(m,n)}(x_2) \\ I^{(m,n)}(x_2) \end{Bmatrix} = \int_A \gamma \begin{Bmatrix} \mathcal{H}_i \\ 1 \end{Bmatrix} x_1^m x_3^n\,\mathrm{d}A \tag{11}$$

Collecting the terms associated with the respective variations δu_2, δf_2, δg_2, $\delta\theta$, and δh, and keeping in mind that these variations have to be arbitrary and independent, Eq. (8) yields the equations of motion and boundary conditions. From the stationary condition $\delta J = 0$ concerning each instant belonging to the interval $[t_0, t_1]$, the equations of motion result as

$$\delta u_2\colon A_1 + \sum_s \delta_D\big(x_2 - x_2^{(s)}\big)\big[-m^{(s)}\big(\ddot{u}_2 + x_3\ddot{f}_2 + x_1 x_3\ddot{g}_2\big)\big] = 0 \tag{12a}$$

$$\delta f_2\colon A_2 + \sum_s \delta_D\big(x_2 - x_2^{(s)}\big)\big[-m^{(s)}\big(x_3\ddot{u}_2 + \big(x_3^2 + K_p^{2(s)}\sin^2\Lambda\big)\ddot{f}_2 + \big(x_1 x_3^2 + x_1 K_p^{2(s)}\sin\Lambda\big)\ddot{g}_2 - K_p^{2(s)}\ddot{\theta}\sin\Lambda\cos\Lambda - E_p^{(s)}\ddot{h}\sin\Lambda\big) + \mathcal{M}^{(s)}\sin\Lambda + m^{(s)} g E_p^{(s)}\sin\Lambda\big] = 0 \tag{12b}$$

$$\delta g_2: A_3 + \sum_s \delta_D\left(x_2 - x_2^{(s)}\right) x_1 \Big[-m^{(s)} \Big(x_3 \ddot{u}_2 + \left(x_3^2 + K_p^{2(s)} \sin^2 \Lambda\right) \ddot{f}_2 + \left(x_1 x_3^2 + x_1 K_p^{2(s)} \sin \Lambda\right) \ddot{g}_2 - K_p^{2(s)} \ddot{\theta} \sin \Lambda \cos \Lambda - E_p^{(s)} \ddot{h} \sin \Lambda \Big) + \mathcal{M}^{(s)} \sin \Lambda + m^{(s)} g E_p^{(s)} \sin \Lambda \Big] = 0 \tag{12c}$$

$$\delta\theta: A_4 + \sum_s \delta_D\left(x_2 - x_2^{(s)}\right) \Big[-m^{(s)} \Big(-K_p^{2(s)} \ddot{f}_2 \sin \Lambda \cos \Lambda - x_1 K_p^{2(s)} \ddot{g}_2 \sin \Lambda \cos \Lambda + \left(x_3^2 + K_p^{2(s)} \cos^2 \Lambda\right) \ddot{\theta} + E_p^{(s)} \ddot{h} \cos^2 \Lambda \Big) - \mathcal{M}^{(s)} \cos \Lambda - m^{(s)} g E_p^{(s)} \cos \Lambda \Big] = 0 \tag{12d}$$

$$\delta h: A_5 + \sum_s \delta_D\left(x_2 - x_2^{(s)}\right) \Big[-m^{(s)} \Big(-E_p^{(s)} \ddot{f}_2 \sin \Lambda - x_1 E_p^{(s)} \ddot{g}_2 \sin \Lambda + E_p^{(s)} \ddot{\theta} \cos \Lambda + \ddot{h} \Big) + \mathcal{L}^{(s)} + m^{(s)} g \Big] = 0 \tag{12e}$$

In addition, the boundary conditions at the wing root and tip are obtained. For a cantilevered wing, the boundary conditions at the root ($x_2 = 0$) are purely geometrical:

$$u_2 = \underline{u}_2 \tag{13a}$$

$$f_2 = \underline{f}_2 \tag{13b}$$

$$g_2 = \underline{g}_2 \tag{13c}$$

$$\theta = \underline{\theta} \tag{13d}$$

$$h = \underline{h} \tag{13e}$$

For a clean wing tip (no tip store), the boundary conditions at $x_2 = l$ are purely statical:

$$\delta u_2: T_{22}^{(0,0)} = \underline{T}_{22}^{(0,0)} \tag{14a}$$

$$\delta f_2: T_{22}^{(0,1)} = \underline{T}_{22}^{(0,1)} \tag{14b}$$

$$\delta g_2: T_{22}^{(1,1)} = \underline{T}_{22}^{(1,1)} \tag{14c}$$

$$\delta\theta: T_{12}^{(0,1)} - T_{23}^{(1,0)} = \underline{T}_{12}^{(0,1)} - \underline{T}_{23}^{(1,0)} \tag{14d}$$

$$\delta h: T_{23}^{(0,0)} = \underline{T}_{23}^{(0,0)} \tag{14e}$$

When considering a tip store, the boundary conditions at $x_2 = l$ change to kinetic ones taking into account mass, inertia properties, and aerodynamics of the tip store,

$$\delta u_2: T_{22}^{(0,0)} = -m^{(T)} \left(\ddot{u}_2 + x_3 \ddot{f}_2 + x_1 x_3 \ddot{g}_2 \right) \tag{15a}$$

$$\delta f_2: T_{22}^{(0,1)} = -m^{(T)} \Big[x_3 \ddot{u}_2 + \left(x_3^2 + K_p^{2(T)} \sin^2 \Lambda\right) \ddot{f}_2 + \left(x_1 x_3^2 + x_1 K_p^{2(T)} \sin \Lambda\right) \ddot{g}_2 - K_p^{2(T)} \ddot{\theta} \sin \Lambda \cos \Lambda - E_p^{(T)} \ddot{h} \sin \Lambda \Big] + \mathcal{M}^{(T)} \sin \Lambda + m^{(T)} g E_p^{(T)} \sin \Lambda \tag{15b}$$

$$\delta g_2: T_{22}^{(1,1)} = x_1 \Big[-m^{(T)} \Big(x_3 \ddot{u}_2 + \left(x_3^2 + K_p^{2(T)} \sin^2 \Lambda\right) \ddot{f}_2 + \left(x_1 x_3^2 + x_1 K_p^{2(T)} \sin \Lambda\right) \ddot{g}_2 - K_p^{2(T)} \ddot{\theta} \sin \Lambda \cos \Lambda - E_p^{(T)} \ddot{h} \sin \Lambda \Big) + \mathcal{M}^{(T)} \sin \Lambda + m^{(T)} g E_p^{(T)} \sin \Lambda \Big] \tag{15c}$$

$$\delta\theta: T_{12}^{(0,1)} - T_{23}^{(1,0)} + x_0 T_{23}^{(0,0)} = -m^{(T)} \Big[-K_p^{2(T)} \ddot{f}_2 \sin \Lambda \cos \Lambda - x_1 K_p^{2(T)} \ddot{g}_2 \sin \Lambda \cos \Lambda + \left(x_3^2 + K_p^{2(T)} \cos^2 \Lambda\right) \ddot{\theta} + E_p^{(T)} \ddot{h} \cos^2 \Lambda \Big] - \mathcal{M}^{(T)} \cos \Lambda - m^{(T)} g E_p^{(T)} \cos \Lambda \tag{15d}$$

$$\delta h: T_{23}^{(0,0)} = -m^{(T)} \Big(-E_p^{(T)} \ddot{f}_2 \sin \Lambda - x_1 E_p^{(T)} \ddot{g}_2 \sin \Lambda + E_p^{(T)} \ddot{\theta} \cos \Lambda + \ddot{h} \Big) + \mathcal{L}^{(T)} + m^{(T)} g \tag{15e}$$

Equations (12–15), in conjunction with Eqs. (9–11), represent the equations governing the aeroelastic equilibrium of advanced composite aircraft wings exhibiting transverse shear flexibility and warping inhibition. In addition, they include arbitrarily distributed external stores in the spanwise and chordwise directions, as well as store aerodynamics. These equations, expressed in terms of the displacement quantities $u_2(x_2; t)$, $f_2(x_2; t)$, $g_2(x_2; t)$, $\theta(x_2; t)$, and $h(x_2; t)$, yield a 10th-order governing system of ordinary differential equations. Upon discarding the influence of the in-plane components of body forces $F_2^{(0,0)}$ as well as in-plane rotatory and inertia terms, i.e., $I^{(0,0)}\ddot{u}_2$, $I^{(0,1)}\ddot{f}_2$, and $I^{(1,1)}\ddot{g}_2$, then $u_2(x_2; t)$ can be expressed in terms of $f_2(x_2; t)$, $g_2(x_2; t)$, $\theta(x_2; t)$, and $h(x_2; t)$ and, therefore, can be eliminated. In this way, the system can be equivalently reduced to an eighth-order differential equation system in terms of $f_2(x_2; t)$, $g_2(x_2; t)$, $\theta(x_2; t)$, and $h(x_2; t)$.

Constitutive Equations

The constitutive equations relating the generalized stress couples $T_{ij}^{(m,n)}$ with the strain measures have been obtained in Ref. 13. To establish trends and to study the basic aeroelastic behavior of the structural configuration, the wing was chosen to be fabricated of a transversely isotropic material. For such a type of anisotropy, the nonzero elastic coefficients intervening in the expressions of the stiffness quantities are

$$\bar{Q}_{11} = \bar{Q}_{22} = E/(1 - \nu^2) \tag{16a}$$

$$\bar{Q}_{12} = E\nu/(1 - \nu^2) \tag{16b}$$

$$\bar{Q}_{66} = G_{12} \left[\equiv \frac{E}{2(1 + \nu)} \right] \tag{16c}$$

$$Q_{44} = Q_{55} = G' \tag{16d}$$

Because of their outstanding thermomechanical properties, materials featuring this type of anisotropy are likely to play a major role in the construction of supersonic and reusable hypersonic flight vehicles.[14, 15]

Numerical Solution of the Static Aeroelastic System

Applying the extended Galerkin method for a numerical solution of the problem, the displacement field is represented as the sum of a finite number of mode shape functions:

$$[f_2(\eta), g_2(\eta), \theta(\eta), h(\eta)]^T = \sum_{j=1}^{n} [F_j, G_j, T_j, H_j]^T \cdot \eta^j \tag{17}$$

where η is the nondimensional spanwise coordinate ($\eta = x_2/l$), whereas F_j, G_j, T_j, and H_j are the modal amplitudes. Because of the structural complexity of the model and to establish trends, strip theory aerodynamics have been employed. However, it should be stressed that the application of the extended Galerkin method allows a three-dimensional integration of the aerodynamic forces and moments along the wing span. Therefore, the sectional lift-curve slope and aerodynamic center remain arbitrary and, thus, may vary from section to section.

For the static case, the aerodynamic terms $\mathcal{L}$ and $\mathcal{M}$ representing the sectional lift and aerodynamic torsional moment are expressed as[16]

$$\mathcal{L}(\eta) = q_n c a_0 \theta_{\text{eff}} \tag{18a}$$

$$\mathcal{M}(\eta) = q_n c e a_0 \theta_{\text{eff}} \tag{18b}$$

where $q_n = \rho_0 V_n^2/2 = q \cos^2 \Lambda$ is the dynamic pressure component normal to the leading edge, and $a_0 \equiv 2\pi \text{AR}/(\text{AR} + 4 \cos \Lambda)$ is the lift-curve slope coefficient corrected to include the effects of a finite wing span and the wing sweep angle Λ, where $\text{AR} = 2l/c$. In Eq. (18), θ_{eff} is the effective sectional angle of attack given by

$$\theta_{\text{eff}} = \theta_0 + \theta - \frac{1}{l} \frac{\partial h}{\partial \eta} \tan \Lambda \tag{19}$$

With θ_0 being the angle of attack of the rigid-wing structure, Eq. (19) including aerodynamic bending/twist coupling describes

the well-known wash-in and wash-out effects of swept-forward and swept-back wing configurations, respectively. Employing Eqs. (17–19) in Eq. (8), an inhomogeneous matrix equation describing the static aeroelastic response of the wing is obtained:

$$[\boldsymbol{A}] \cdot [\boldsymbol{s}] = [\boldsymbol{r}] \tag{20}$$

The matrix $\boldsymbol{A}$ is composed of the (real) stiffness matrix of the wing but also contains the (real) aerodynamic influence quantities in terms of the dynamic pressure q_n, whereas $\boldsymbol{s}$ is the solution vector with $\boldsymbol{s} = [F_1 \cdots F_n, G_1 \cdots G_n, T_1 \cdots T_n, H_1 \cdots H_n]^T$. The right-hand vector $\boldsymbol{r}$ incorporates the inhomogeneous part of the aerodynamic forces associated with the angle of attack of the rigid wing and the influence of the external stores. To obtain the divergence pressure, the determinant of matrix $\boldsymbol{A}$ has to be calculated, yielding a characteristic polynomial in q_n. The smallest positive value of q_n fulfilling the condition $\det \boldsymbol{A} = 0$ represents the divergence pressure $(q_n)_{\text{div}}$. Because there is no contribution of the external stores to the matrix $\boldsymbol{A}$, it now becomes evident that the influence of the stores on the wing's divergence speed is immaterial. Figure 2 shows calculated divergence pressures for two aspect ratios and selected values of the transverse shear flexibility parameter $R = E/G'$. Results related to the static aeroelastic response of the clean wing represented in terms of the ratio $\theta_{\text{eff}}/\theta_0$ reveal that transverse shear flexibility considerably affects the static response in the subcritical flight regime, especially for the case of forward-swept wings. Because identical results were previously obtained via the Laplace transform method,[13] they are not displayed here. As a consequence,

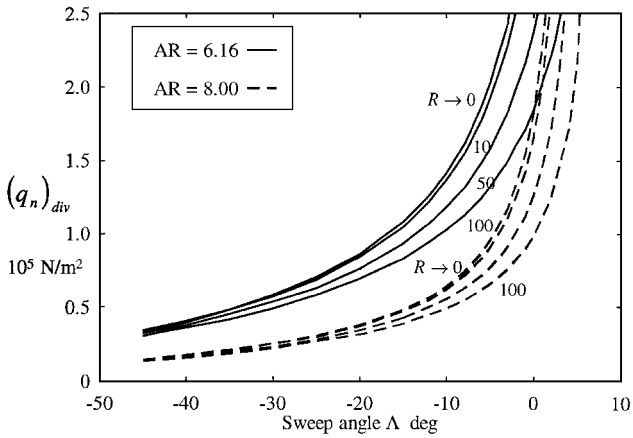

Fig. 2 Variation of normal divergence pressure $(q_n)_{\text{div}}$ vs sweep angle Λ for different ratios of $R = E/G'$.

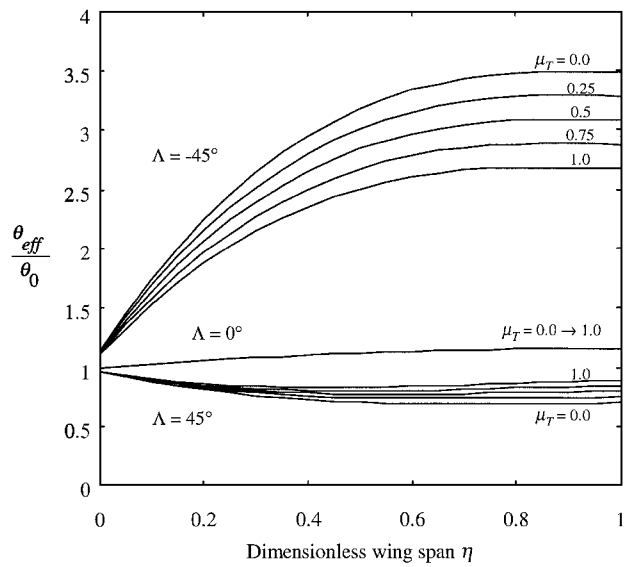

Fig. 3 Spanwise distribution of the normalized effective angle of attack $\theta_{\text{eff}}/\theta_0$ for different sweep angles Λ and selected ratios of $\mu_T = m_{\text{tipstore}}/m_{\text{wing}}$, where $R = 100$, AR = 6.16, and $q_n/(q_n)_{\text{div}} = 0.7$.

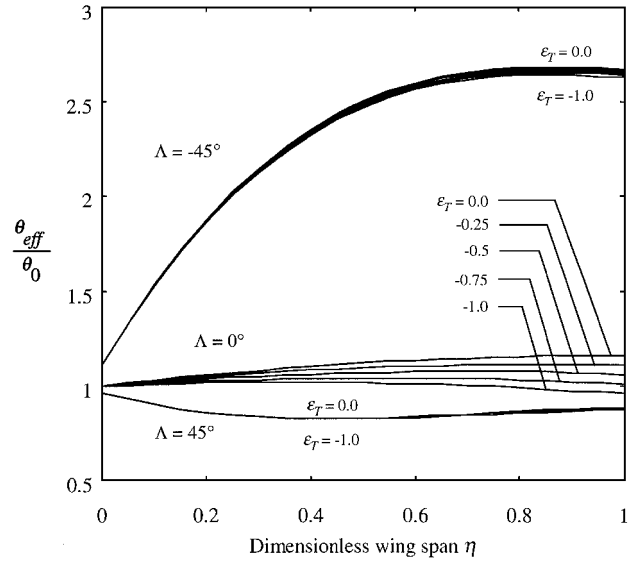

Fig. 4 Spanwise distribution of the normalized effective angle of attack $\theta_{\text{eff}}/\theta_0$ for different sweep angles Λ and selected ratios of $\varepsilon_T = E_P/c$, where $R = 100$, AR = 6.16, and $q_n/(q_n)_{\text{div}} = 0.7$.

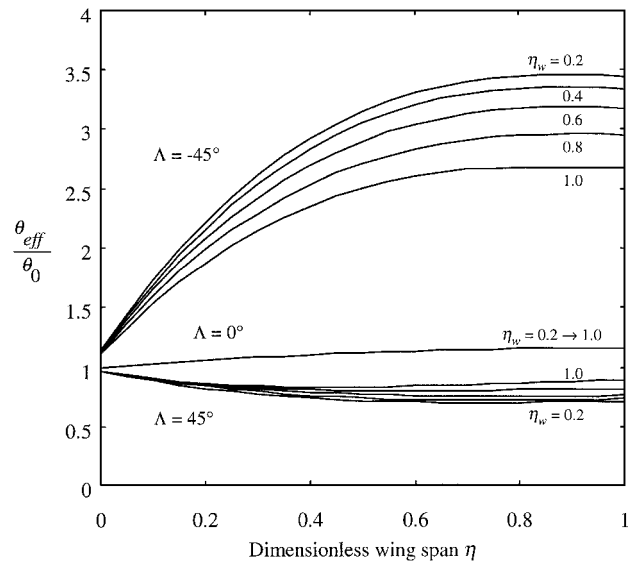

Fig. 5 Spanwise distribution of the normalized effective angle of attack $\theta_{\text{eff}}/\theta_0$ for different sweep angles Λ and selected ratios of $\eta_W = x_{2\,\text{wingstore}}/l$, where $R = 100$, AR = 6.16, and $q_n/(q_n)_{\text{div}} = 0.7$.

for the following investigations of the static aeroelastic behavior, the transverse shear flexibility measure was set to $R = E/G' = 100$.

Figure 3 shows the influence of a tip store in terms of $\mu_T = m_{\text{tipstore}}/m_{\text{wing}}$. Because of a decrease in the upward bending deflection caused by the store mass, the wash-in as well as wash-out effects are attenuated. To prevent dynamic aeroelastic instability, the center of gravity of the store usually is moved forward of the elastic axis of the wing. For the static case, this results in a torsional moment that tends to attenuate the wing's static aeroelastic response. The influence of this moment is most pronounced for straight wings. For swept wings, it is split into a contribution to wing torsion and bending (Fig. 4). The influence of the spanwise store location is shown in Fig. 5 in terms of $\eta_W = x_{2\,\text{wingstore}}/l$.

Numerical Solution of the Dynamic Aeroelastic System

For simulation of the dynamic system, the unknown functions are represented as

$$[f_2(\eta; t), g_2(\eta; t), \theta(\eta; t), h(\eta; t)]^T = \sum_{j=1}^{n} [F_j, G_j, T_j, H_j]^T \cdot \eta^j \cdot e^{i\omega t} \tag{21}$$

In the dynamic case, the aerodynamic terms $\mathcal{L}$ and $\mathcal{M}$, representing the sectional lift and aerodynamic torsional moment, are expressed as[16]

$$\mathcal{L}(\eta, t) = -\pi\rho\omega^2 b^3 \left\{ \frac{h}{b} L_{hh} + \frac{1}{l}\frac{\partial h}{\partial \eta} L_{hh'} + \theta L_{h\theta} + b\frac{1}{l}\frac{\partial \theta}{\partial \eta} L_{h\theta'} \right\} \tag{22a}$$

$$\mathcal{M}(\eta, t) = \pi\rho\omega^2 b^4 \left\{ \frac{h}{b} M_{\theta h} + \frac{1}{l}\frac{\partial h}{\partial \eta} M_{\theta h'} + \theta M_{\theta\theta} + b\frac{1}{l}\frac{\partial \theta}{\partial \eta} M_{\theta\theta'} \right\} \tag{22b}$$

In Eq. (22), $L_{hh}, L_{hh'}, \ldots, M_{\theta\theta'}$ are the aerodynamic coefficients as displayed in Ref. 16. For the Theodorsen function $C(k)$, the approximation given in Ref. 17 was used:

$$\begin{aligned} C(k) &= F(k) + iG(k) \\ &= \frac{0.021573 + 0.210400k + 0.512607k^2 + 0.500502k^3}{0.021508 + 0.251239k + 1.035378k^2 + k^3} \\ &\quad - i\frac{0.001995 + 0.327214k + 0.122397k^2 + 0.000146k^3}{0.089318 + 0.934530k + 2.481481k^2 + k^3} \end{aligned} \tag{23}$$

with k the reduced frequency $k = \omega b/V_n = \omega b/(V\cos\Lambda)$. This finally leads to a complex eigenvalue problem expressed in matrix form as

$$[\boldsymbol{A}] - \omega^2[\boldsymbol{B}] = \boldsymbol{0} \tag{24}$$

where $\boldsymbol{A}$ is the (real) stiffness matrix of the wing and $\boldsymbol{B}$ is the (complex) matrix representing the inertia terms of wing and external stores, as well as the complex aerodynamic parameters. The real part of the complex quantity ω represents the circular frequency of oscillation, whereas its imaginary part is the damping factor δ. The implemented solution methodology is based on the inversion of matrix $\boldsymbol{B}$ and subsequent calculation of complex eigenvalues and eigenvectors of the system matrix $\boldsymbol{AB}^{-1}$. The flutter speed is calculated in a fast converging iteration process rendering zero the imaginary (damping) part of the eigenvalues. Unlike in other models of similar structural complexity, the solution procedure neither involves a trial and error process[3,18] nor requires enforcement of convergence of the solution toward the flutter speed of the system.[11]

Free Vibration

The free vibration behavior of shear deformable wings carrying external stores can be obtained as a byproduct of the dynamic analysis described in the preceding section. For this purpose, the airflow speed was set equal to zero, rendering the inertia matrix $\boldsymbol{B}$ real and stating a self-adjoint eigensystem with real eigenvalues. The influence of the transverse shear flexibility of the material is shown in Fig. 6. As is shown, neglecting transverse shear flexibility in the case of composite materials leads to an overestimation of vibration frequencies. Because of an external store on the wing, the vibration frequencies are further decreased. Figure 7 shows first and second bending and torsional frequencies for a transversely flexible wing vs the store mass for three different spanwise store positions $\eta_S = x_{2\,\text{store}}/l$.

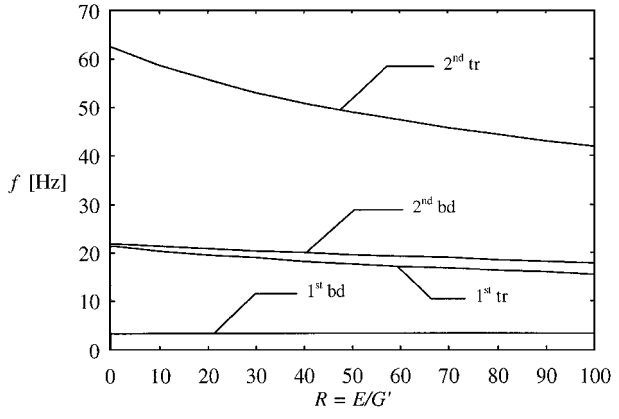

Fig. 6 Influence of transverse shear flexibility in terms of $R = E/G'$ on vibration frequencies of first and second natural bending and torsional modes.

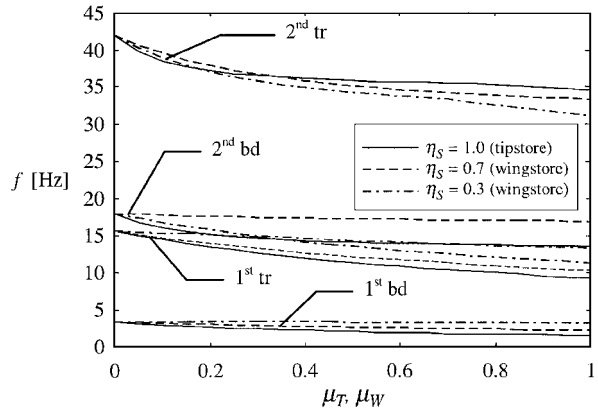

Fig. 7 Influence of dimensionless store mass on vibration frequencies of first and second natural bending and torsional modes of a transversely flexible wing, $R = 100$.

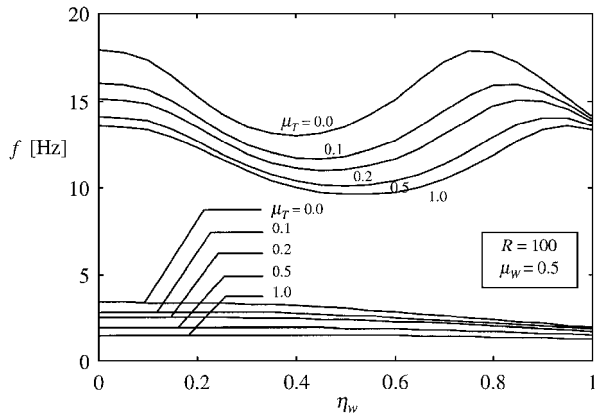

Fig. 8 Influence of dimensionless tipstore mass μ_T and spanwise wing store location η_w on vibration frequencies of first and second natural bending modes, $R = 100$ and $\mu_W = 0.5$.

Figure 8 shows the vibration behavior of a wing carrying a wing and a tip store. Vibration frequencies are lowered by increasing the tip mass and moving outward the underwing store. However, moving the wing store toward the node line of the second bending mode results in an important increase of the vibration frequency of this mode. As can be inferred from Fig. 8, the node line of the second bending mode also is shifted outward by increasing the tip mass. The first and second torsional vibration modes of the wing exhibit a similar behavior. This trend is consistent with the one experimentally obtained by Runyan and Sewall.[19]

Dynamic Aeroelastic Instability (Flutter)

For a nonzero airflow speed, matrix $\boldsymbol{B}$ becomes complex causing the eigenvalues of the system to become complex quantities. To verify the accuracy of the flutter analysis, comparisons for several test cases were conducted. The first comparison was made with Goland's[20] cantilevered wing of AR = 6.67 with the subsequently appended correction of the results in Ref. 21. As shown in Table 1 (Refs. 10 and 20–22), the predictions provided by the present approach are in excellent agreement with Goland's exact results. As another test case, a straight wing of AR = 6.16 with attached tip weights[21] was investigated. In the calculations, two different chordwise positions of the center of gravity of the store were considered, $\varepsilon_T = 0.0$ (case I) and $\varepsilon_T = 0.1$ (case II). The original flutter investigation in Ref. 21 included the free body motion of the fuselage, which is not subject of the present calculations. Nevertheless, flutter speed prediction for the first torsional mode for cases I and II is very accurate (Table 1).

Table 1 Comparison of calculated flutter speeds for a uniform cantilevered wing of aspect ratio 6.67 (Refs. 20 and 21) and a uniform wing with tip weights of aspect ratio 6.16 (Ref. 21)

Program or reference	Description	Flutter speed, km/h	Flutter frequency, Hz
References 20 and 21	Exact analysis	494	11.25
Present	Extended Galerkin method ($n=4$)	492.3	12.06
Present	Extended Galerkin method ($n=7$)	493.6	12.02
COMBOF[10]	10 finite difference stations	484.2	11.20
COMBOF[10]	25 finite difference stations	483.1	11.27
SADSAM[22]	1 finite element	447.1	——
SADSAM[22]	10 finite elements	472.5	——
Reference 21 (case I)	Exact analysis	1054	3.05
Present	Extended Galerkin method ($n=4$)	1057.8	3.45
Present	Extended Galerkin method ($n=7$)	1055.1	3.46
COMBOF[10]	31 finite difference stations	1049	3.05
SADSAM[22]	10 finite elements	1049	3.01
Reference 11	Exact analysis	1042.8	3.09
Reference 21 (case II)	Exact analysis	826	3.05
Present	Extended Galerkin method ($n=4$)	836.3	3.30
Present	Extended Galerkin method ($n=7$)	835.8	3.26
COMBOF[10]	31 finite difference stations	821	3.02
SADSAM[22]	10 finite elements	837	3.00

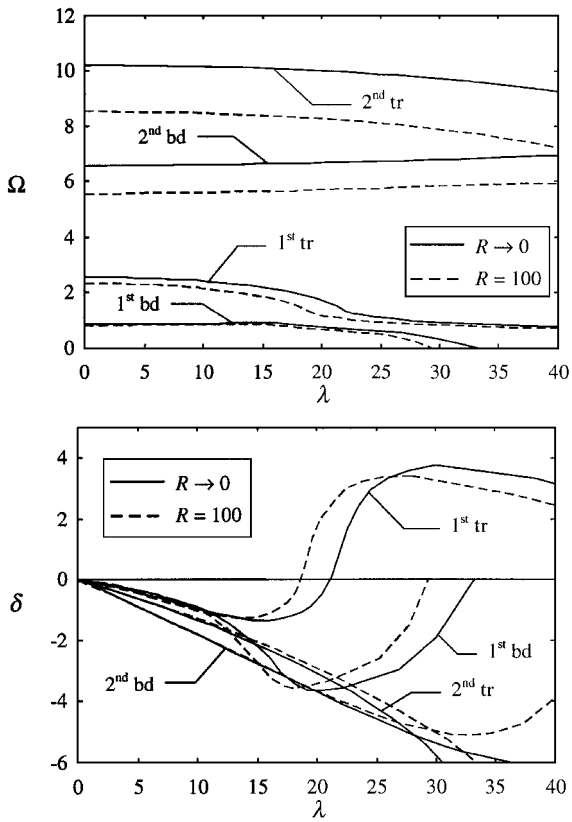

Fig. 9 Frequency and damping of the fundamental aeroelastic modes (first and second bending and torsion) vs flight speed parameter $\lambda = V/b\omega_h$ for Goland and Luke's unswept wing[21] including warping inhibition, case I $\varepsilon_T = 0.0$.

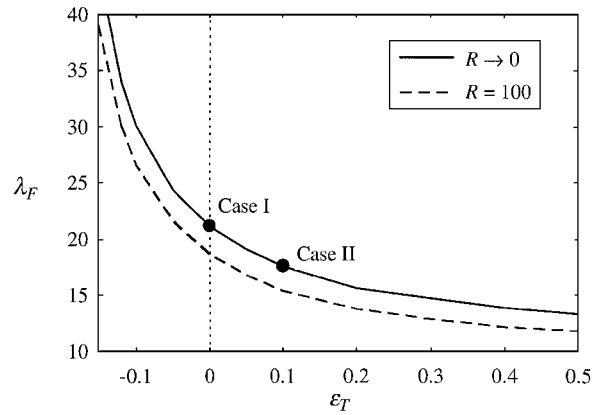

Fig. 10 Effect of chordwise position of store center of gravity on flutter speed parameter $\lambda_F = V_F/b\omega_h$ for a classical ($R \to 0$) and shear deformable ($R = 100$) unswept wing: ●, Goland and Luke's unswept wing.[21]

Figure 9 shows frequency and damping of the fundamental aeroelastic modes (first and second bending and torsion) vs the flight speed for Goland and Luke's[21] unswept wing carrying a tip weight (case I, $\varepsilon_T = 0.0$). Flutter occurs in the classical way as binary bending/torsion flutter due to frequency coalescence and vanishing aerodynamic damping of the first torsional mode at a flight speed of 1055 km/h. In Refs. 10 and 11, it was observed that the first bending branch interacts with the rigid-body mode and flutters at an even lower speed (994 km/h). Because free body motion of the fuselage was discarded in this investigation, there is no such interaction, and as a consequence, the first torsional mode yields the lowest flutter speed. In the present calculations, warping inhibition of the cantilevered wing structure is taken into account. For this reason, flutter of the second bending mode, which was observed by Housner and Stein[10] to be the most critical mode of instability (943 km/h), occurs at very high air speeds.[11] Inclusion of the warping terms does not influence the stability behavior of the first bending and torsional modes.

To emphasize the influence of the transverse shear flexibility of the material on flutter behavior, Fig. 9 also shows frequency and damping for the same structural configuration, but exhibiting flexibility in transverse shear ($R = E/G' = 100$). Besides an important decrease in structural damping for all modes, flutter speed is decreased by more than 12% with respect to the structure featuring infinite rigidity in transverse shear (Kirchhoff's theory, $R = E/G' \to 0$). For the same wing, the influence of the chordwise position of the center of gravity of the store was investigated. Figure 10 shows that, as the location of the center of gravity of the store is moved aft ($\varepsilon_T > 0.0$), the flutter speed drops significantly. Moving the center of gravity of the tip weight forward ($\varepsilon_T < 0.0$) dramatically increases the flutter speed. The influence of the chordwise position of the store center of gravity on the flutter frequency is much less pronounced.

Figures 11 and 12 show the variation of flutter speed and frequency vs the wing sweep angle Λ. The trend of variation of the flutter speed, as shown in Fig. 11, is similar to the one in Refs. 11 and 23. By attaching an external store of 70% of the wing mass ($\mu_w = 0.7$) to the wing, located at 50% of the wing half-span ($\eta_W = 0.5$), the flutter speed is decreased, but shows the same trend of variation with the sweep angle Λ. From the static system, it was derived that the divergence speed of the wing should not be influenced by the attachment of external stores. As it can be seen from Fig. 11,

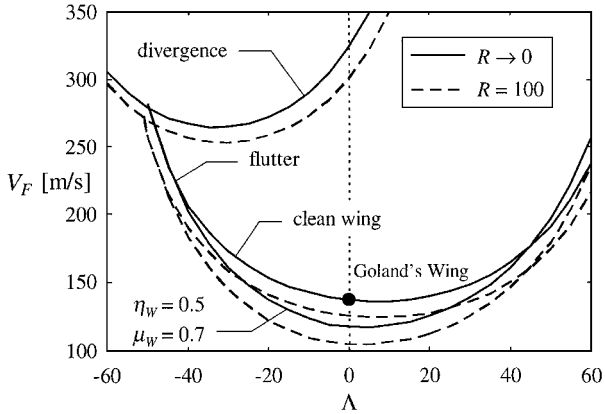

Fig. 11 Effect of sweep angle Λ on flutter speed V_F for a classical ($R \to 0$) and shear deformable ($R = 100$) wing, $\mu_w = m_{\text{wingstore}}/m_{\text{wing}}$, $\eta_w = x_{2\,\text{wingstore}}/l$: ●, Goland's[20] and Goland and Luke's[21] unswept wing.

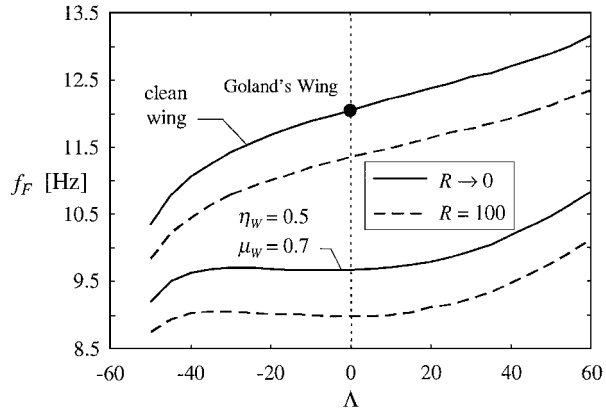

Fig. 12 Effect of sweep angle Λ on flutter frequency f_F for a classical ($R \to 0$) and shear deformable ($R = 100$) wing, $\mu_w = m_{\text{wingstore}}/m_{\text{wing}}$, $\eta_w = x_{2\,\text{wingstore}}/l$: ●, Goland's[20] and Goland and Luke's[21] unswept wing.

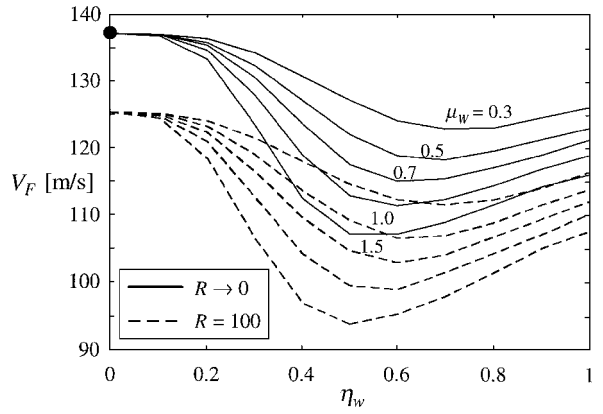

Fig. 13 Effect of spanwise store location η_W on flutter speed V_F for classical ($R \to 0$) and shear deformable ($R = 100$) wings, $\mu_w = m_{\text{wingstore}}/m_{\text{wing}}$: ●, Goland's[20] and Goland and Luke's[21] unswept wing.

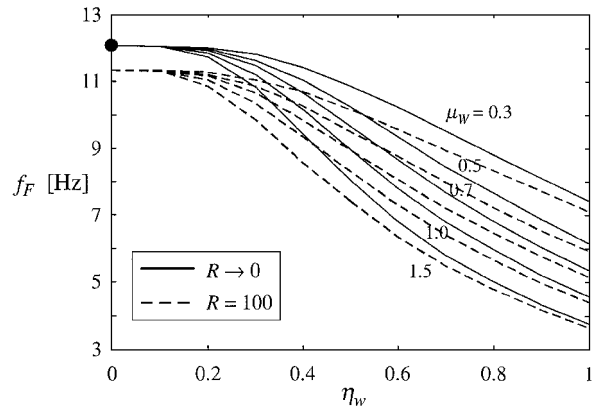

Fig. 14 Effect of spanwise store location η_W on flutter frequency f_F for classical ($R \to 0$) and shear deformable ($R = 100$) wings, $\mu_w = m_{\text{wingstore}}/m_{\text{wing}}$: ●, Goland's[20] and Goland and Luke's[21] unswept wing.

divergence and flutter speed of the wing coincide at a sweep angle of $\Lambda = -51$ deg for both cases, $\mu_w = 0.7$ and 0.0. In this case and for even smaller sweep angles ($\Lambda < -51$ deg) the solution of the dynamic system also yields that frequency and damping of the first torsional mode tend toward zero, thus indicating static aeroelastic instability (divergence).

The results shown in Fig. 11 are not typical. For most structural configurations, divergence is the critical mode of instability of a forward-swept wing. In the case of Goland's[20] wing, due to the small ratio of $GJ/EI_b = 0.101$, flutter is also the more critical aeroelastic instability mode for very high forward sweep angles. An identical behavior was also observed by Lottati[24] and is extended herein to a wing carrying external stores and exhibiting flexibility in transverse shear. Figure 12 indicates that the flutter frequency rapidly tends toward zero when approaching a sweep angle of $\Lambda = -51$ deg. The same behavior is exhibited by a transverse shear deformable wing ($R = 100$).

Figure 13 shows the influence of the spanwise location of a wing store for several mass ratios of $\mu_w = m_{\text{wingstore}}/m_{\text{wing}}$ and two transverse shear flexibility ratios of R. Despite a higher overall level of the flutter speed for the transversely rigid structure, it may be dramatically reduced even for small ratios of μ_w. The flutter speed drops as the store is moved from the base to the wing midspan, then increases as the wing tip is approached. The observed behavior is in excellent agreement with previously published results by Runyan[9] and with experimental ones by Runyan and Sewall.[19] However, it should be stressed that the work in Refs. 9 and 19 was done for unswept metallic wings. The presented model constitutes an extension toward the consideration of composite swept-wing configurations. The decrease in flutter frequency for both cases is shown in Fig. 14.

Ongoing activities are intended to evaluate the implications of the free body motion of the fuselage, which in some instances may influence aeroelastic instability of forward-swept wings.[25] This issue will be approached in conjunction with the effects of external stores. Inclusion of the free body motion has been shown in Ref. 26 by changing the geometrical boundary conditions at the wing root into kinetic ones, taking into account mass and inertia of the fuselage. In the present analysis, the stores are regarded to be rigidly attached to the wing structure. Therefore, the consideration of pylon flexibility will be an important step toward a more realistic representation of store influence on wing aeroelasticity. Although the effects of store aerodynamics may be negligible in many cases, some examples are presented by Turner[27] for which store aerodynamics may be significant. As a result, store aerodynamics will also be incorporated in forthcoming works.

Conclusions

An encompassing structural model of composite aircraft wings exhibiting transverse shear flexibility and warping inhibition, as well as incorporating arbitrarily distributed stores, was developed. The model, intended to be used in aeroelastic analyses, has demonstrated its applicability to study the static and dynamic aeroelasticity of complex wing/store configurations. Results obtained for Goland's and for Goland and Luke's wings via the extended Galerkin's method and employment of three-dimensional strip theory aerodynamics show very good agreement with solutions given by other authors and obtained via completely different approaches such as exact solution methodologies, finite difference, and finite element models. These results are also identified in Figs. 10–14. The accuracy of the model is underlined by comparison with theoretical and experimental results for unswept metallic wings.

The assumption of a non-shear deformable structure ($R = E/G' \to 0$) underestimates subcritical aeroelastic twist and overestimates vibration frequencies, divergence, and flutter speeds and frequencies. For this reason, to obtain reliable results, transverse shear

flexibility always has to be considered. The beneficial effect of external stores on the wing's static aeroelastic response consists of attenuating the wash-in effect of forward-swept wings. Because divergence is only influenced by wing stiffness parameters, the effect of external stores on the divergence speed has been shown to become immaterial.

For free vibration and flutter, store mass and location have a great influence on natural frequencies, mode shapes, and flutter speed and frequency. Depending on the wing/store configuration, the implications of external stores on flutter speed may be of beneficial or detrimental nature. As displayed in several figures, this behavior is also dramatically influenced by the transverse shear flexibility of the wing structure.

Acknowledgment

Frank H. Gern wishes to thank the German Research Society (Deutsche ForschungsgemeinschaftDFG) for funding his research work under research Grant Ge 923/1-1. This support is highly appreciated.

References

[1]Försching, H., "New Ultra High Capacity Aircraft (UHCA)—Challenges and Problems from an Aeroelastic Point of View," *ZFW, Zeitschrift für Flugwissenschaften und Weltraumtechnik [Journal of Flight Sciences and Aerospace Research]*, Vol. 18, No. 4, 1994, pp. 219–231.

[2]Weisshaar, T. A., "Aeroelastic Tailoring of Forward Swept Composite Wings," *Journal of Aircraft*, Vol. 18, No. 8, 1981, pp. 669–676.

[3]Karpouzian, G., and Librescu, L., "Nonclassical Effects on Divergence and Flutter of Anisotropic Swept Aircraft Wings," *AIAA Journal*, Vol. 34, No. 4, 1996, pp. 786–794.

[4]Bhatia, K. G., Nagaraja, K. S., and Ruhlin, C. L., "Winglet Effects on the Flutter of Twin-Engine-Transport-Type Wing," AIAA Paper 84-0905, May 1984.

[5]Reed, W. H., Foughner, J. T., and Runyan, H. L., "Decoupler Pylon: A Simple Effective Wing/Store Flutter Suppressor," *Journal of Aircraft*, Vol. 17, No. 3, 1980, pp. 206–211.

[6]*Specialists Meeting on Wing-With-Stores Flutter*, CP-162, AGARD, 1975.

[7]Försching, H., and Senft, A., "A Parametric Study of the Aeroelastic Stability of a Binary Wing-With-Engine Nacelle Flutter System in Incompressible Flow," *ZFW, Zeitschrift für Flugwissenschaften und Weltraumtechnik [Journal of Flight Sciences and Aerospace Research]*, Vol. 16, No. 2, 1994, pp. 77–87.

[8]Desmarais, R. N., and Reed, W. H., "Wing/Store Flutter with Nonlinear Pylon Stiffness," *Journal of Aircraft*, Vol. 18, No. 11, 1981, pp. 984–987.

[9]Runyan, H. L., "Effect of a Flexibly Mounted Store on the Flutter Speed of a Wing," NASA CR-159245, April 1980, p. 22.

[10]Housner, J. M., and Stein, M., "Flutter Analysis of Swept-Wing Subsonic Aircraft with Parameter Studies of Composite Wings," NASA TN-D-7539, Sept. 1974.

[11]Lottati, I., "Aeroelastic Stability Characteristics of a Composite Swept Wing with Tip Weights for an Unrestrained Vehicle," *Journal of Aircraft*, Vol. 24, No. 11, 1987, pp. 793–802.

[12]Librescu, L., *Elastostatics and Kinematics of Anisotropic and Heterogeneous Shell-Type Structures*, Noordhoff, Leyden, The Netherlands, 1975.

[13]Karpouzian, G., and Librescu, L., "Comprehensive Model of Anisotropic Composite Aircraft Wings Suitable for Aeroelastic Analysis," *Journal of Aircraft*, Vol. 31, No. 3, 1994, pp. 703–712.

[14]Garber, A. M., "Pyrolitic Materials for Thermal Protection Systems," *Aerospace Engineering*, Vol. 22, No. 1, 1963, pp. 126–137.

[15]Woods, R. H., "Pyrolitic Graphite for High Pressure, High Temperature Applications," AIAA Paper 76-605, Feb. 1976.

[16]Bisplinghoff, R. L., Ashley, H., and Halfman, R. L., *Aeroelasticity*, Addison–Wesley, Reading, MA, 1955.

[17]AGARD, *Manual on Aeroelasticity*, Vol. 6, edited by J. W. Jones, 1961.

[18]Scanlan, R. H., and Rosenbaum, R., *Aircraft Vibration and Flutter*, Dover, New York, 1954.

[19]Runyan, H. L., and Sewall, J. L., "Experimental Investigation of the Effects of Concentrated Weights on Flutter Characteristics of a Straight Cantilever Wing," NACA TN-1594, Nov. 1947.

[20]Goland, M., "The Flutter of a Uniform Cantilever Wing," *Journal of Applied Mechanics*, Vol. 12, No. 4, 1945, pp. A-197–A-208.

[21]Goland, M., and Luke, Y. L., "The Flutter of a Uniform Wing with Tip Weights," *Journal of Applied Mechanics*, Vol. 15, No. 1, 1948, pp. 13–20.

[22]Peterson, L., "SADSAM User's Manual, MSR-10," McNeal–Schwendler Corp., Santa Monica, CA, Dec. 1970.

[23]Barmby, J. G., Cunningham, H. J., and Garrick, I. E., "Study of Effects of Sweep on the Flutter of Cantilever Wings," NACA Rept. 1014 (supersedes NACA TN 2121), Sept. 1951.

[24]Lottati, I., "Flutter and Divergence Aeroelastic Characteristics for Composite Forward Swept Cantilevered Wing," *Journal of Aircraft*, Vol. 22, No. 11, 1985, pp. 1001–1007.

[25]Rodden, W. P., "Comment on General Formulation of the Aeroelastic Divergence of Composite Swept-Forward Wing Structures," *Journal of Aircraft*, Vol. 26, No. 7, 1989, pp. 694–696.

[26]Gern, F. H., and Librescu, L., "Modeling and Aeroelasticity of Advanced Aircraft Wings Carrying External Stores," *Fluid-Structure Interaction, Aeroelasticity, Flow-Induced Vibration and Noise*, AD-Vol. 53-3, edited by P. P. Friedmann and M. P. Païdoussis, American Society of Mechanical Engineers, New York, 1997, pp. 185–195.

[27]Turner, C. D., "Effect of Store Aerodynamics on Wing/Store Flutter," *Journal of Aircraft*, Vol. 19, No. 7, 1982, pp. 574–580.

A. Berman
Associate Editor